ISSN (Print) : 2320 – 3765
ISSN (Online): 2278 – 8875

International Journal of Advanced Research in Electrical, Electronics and Instrumentation Engineering

(An ISO 3297: 2007 Certified Organization)

Vol. 4, Issue 4, April 2015

Study of SVM Based Controller for Grid Connected Wind Turbine

Vinod.S [1], S.Prakash[*2]

Assistant Professor, Dept. of EEE, Jerusalem College of Engineering, Chennai, Tamil Nadu, India[1]

Assistant Professor, Dept. of EEE, Bharath University, Chennai, Tamil Nadu, India[2]

[*] Corresponding Author

ABSTRACT: Extracting as much as wind energy as possible and feeding the grid with high quality power are the two main targets for the grid connected wind turbine system. This paper proposes the design of an efficient controller for the 3.2KW wind turbine which grabs the maximum power from the available wind. The 3.2 KW wind turbine system provides DC voltage and this DC voltage is then converted to constant three phase 230V 50 Hz AC by using the converter and inverter systems.

Neutral Point Clamped Inverter (NPC), Space Vector Modulation (SVM), wind energy conversion, wind power, grid connected wind turbine system, variable speed wind turbine, step up DC-DC converter.

I. INTRODUCTION

The future trend of wind energy conversion systems is to draw the maximum power from the available wind. Unfortunately this is not possible with high capacity wind turbine, as they can be rotated only for a particular speed. The wind turbine system stated here is a 3.2 KW wind turbine which is allowed to rotate at any speed to grab the maximum power from the available wind. The size of the wind turbine system is small, as a result they can be placed on the roof tops and de-regulation of power can be done. This wind turbine system incorporated with a rectifier provides the rectified DC voltage and this DC is converted into constant three phase 230V AC by using the converter and inverter systems.

This paper reviews the major applications of power electronics for wind power conversion systems, and it is organized as follows. Section II briefs about the wind energy conversion system, the modern power electronics and the applications of power electronics for wind turbines are presented. Section III describes about the variable DC to fixed DC step up converter. Section IV discusses the design of Neutral Point Clamped Inverter. Section V presents the Space Vector Modulation control scheme for the Inverter. Section VI describes the simulation circuits. Section VII proposes the prototype design of Converter and Space Vector Modulated Inverter system. Finally in Section VIII, the conclusions are drawn and the future trends are illustrated.

II. WIND ENERGY CONVERSION SYSTEM

The main components of a wind turbine system are illustrated in Fig.1, including a turbine blade, generator, rectifier, power electronic system **[1]**. Wind turbines capture the power from wind by means of turbine blades and convert it to mechanical power. Wind at any speed can be capture and it is transformed into AC voltage with any frequency. Since the obtained AC voltage can be of any frequency the power limitation using pitch control, yaw control and gear box control can be avoided [2]. Thus the size and the weight of the system is reduced which forms to be a great advantage for this system [3]. Hence the system can also be installed in rooftops.

The obtained AC voltage from the wind turbine system is converted into DC voltage using the inbuilt rectifier system. The obtained DC is of low voltage [4]. This low voltage variable DC is fed to the DC/DC Boost converter. The

ISSN (Print) : 2320 – 3765
ISSN (Online): 2278 – 8875

International Journal of Advanced Research in Electrical, Electronics and Instrumentation Engineering

(An ISO 3297: 2007 Certified Organization)

Vol. 4, Issue 4, April 2015

Boosted constant DC voltage obtained from the converter is then feed to the Inverter to obtain AC voltage with a frequency of 50Hz [5].

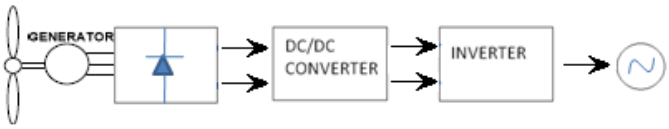

Fig.1. Wind turbine grid connected system

The electrical protection system of a wind turbine system protects the wind turbine as well as secures the safe operation of the network.

III. STEP UP DC-DC CONVERTER

The step-up DC-DC converter is shown in the Fig.2. Compared to the conventional boost converter, there are extra secondary windings for the boost inductor, rectification diode D_2 and filtering capacitor C_2. The proposed converter is boost-flyback connected in series to increase the efficiency and output voltage gain with the integrated coupled inductor [6]. By cascading the output voltage V_{C1} of the boost converter and the output voltage V_{C2} of the flyback converter, high output voltage V_0 is easily obtained. In addition, there is low voltage stress on the power switch and diode as well as on the output capacitors compared to that for conventional boost converters [7]. The low side capacitor C_1 functions as output capacitor and snubber capacitor, to suppress the voltage spike on S_1 during the turn-off transient period, which recycles the leakage energy in the coupled inductor [8]. A power switch S_1 with low voltage rating is used to reduce conduction loss, and as a result the overall efficiency is significantly improved.

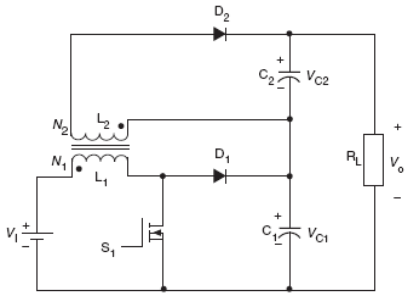

Fig.3. Equivalent circuit of DC-DC converter

The step up converter is a combination of conventional converter and flyback converter and is assumed to be operated in continuous conduction mode. The switch S_1 is turned ON at t_0, the voltage across the magnetizing inductance is equal to V_1 and the magnetizing current will increase with a slope of V_1/L_m. Diode D_1 is reversed-biased and C_1 and C_2 supply energy to load. The peak magnetizing current is obtained at the time instant t_1 when the switch S_1 is turned OFF [9]. The magnetizing current charges the parasitic capacitor C_0 of the MOSFET, and the voltage increases until time instant t_2. At t_2, diodes D_1 and D_2 start to conduct [10].

When the diode D1 starts to conduct, a large portion of the magnetizing current will flow into the capacitor C1 of the active clamp owing to the leakage inductance in the output loops [11]. Thus current id1 continues to decrease and id2 continues to increase. At the same time, the current id1 falls, this is complementary to id2. At the end of the mode, iC1 decreases to zero, and energy is discharged from C1 to supply the load current. The current id2 is charging C2 and at the same time supplying the load current [12].

ISSN (Print) : 2320 – 3765
ISSN (Online): 2278 – 8875

International Journal of Advanced Research in Electrical, Electronics and Instrumentation Engineering

(An ISO 3297: 2007 Certified Organization)

Vol. 4, Issue 4, April 2015

IV. NEUTRAL POINT CLAMPED INVERTER

The three-level NPC inverter is shown below in Fig.4. With this inverter topology, it is possible to produce three voltage levels at the output of inverter leg, namely, $V_{dc}/2$, 0 and $2V_{dc}/2$. The performance of this three level inverter can be made efficient by controlling it using the Space Vector Modulation [4] , [13].

As shown in Fig.4, only one active voltage source of $V_{dc}/2$ is used [2]. The rated DC link voltage can be obtained by switching the voltage source between the top capacitor (C_1) and the bottom capacitor (C_2) with a duty ratio of 0.5 [14]. The capacitors will charge to $V_{dc}/2$ with a constant frequency irrespective of the load currents [7]. Therefore the load current flowing through the capacitors will not create any neutral-point fluctuations. Here, the diode bridge rectifier and filter capacitor C_3 is used as an input voltage source. To switch the voltage source between the capacitors C_1 and C_2, two extra switches and two extra diodes are required, as shown.

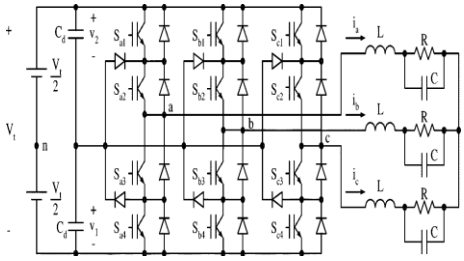

Fig.4. Equivalent circuit of NPC inverter

V. THE SPACE VECTOR MODULATION

The Space Vector is defined as the vector 'V_s' having a magnitude of "$3/2V_m$" and rotates in space at a frequency of "ω" radians per second. Space Vector Modulation (SVM) refers to a special switching sequence of the upper three transistors of a three phase power inverter. It has been shown to generate less harmonic distortion in the output voltage which is supplied to the grid [3].

Five steps can be identified to implement the space vector modulation for inverters
i. Definition of the possible switching vectors in the output voltage space.
ii. Identification of the separation planes between the sectors in the output voltage space
iii. Identification of the boundary planes in the output voltage space.
iv. Obtaining of the decomposition matrices
v. Definition of the switching sequence.

A. ANALYSIS OF SAPCE VECTOR MODULATON

The SVPWM method considers this interaction of the phase and optimizes the harmonic content of the three phase isolated neutral load [5]. The three phase sinusoidal and balance voltages equations are given as,

$$\bar{v}_{an} = V_m \cos(2\pi f \cdot t) \quad (1)$$

$$\bar{v}_{bn} = V_m \cos(2\pi f \cdot t - \frac{2\pi}{3}) \quad (2)$$

$$\bar{v}_{cn} = V_m \cos(2\pi f \cdot t - \frac{4\pi}{3}) \quad (3)$$

$$\bar{V} = \frac{2}{3}\left[v_{an} + a v_{bn} + a^2 v_{cn} \right] \quad (4)$$

ISSN (Print) : 2320 – 3765
ISSN (Online): 2278 – 8875

International Journal of Advanced Research in Electrical, Electronics and Instrumentation Engineering

(An ISO 3297: 2007 Certified Organization)

Vol. 4, Issue 4, April 2015

Thus in SVM the voltages across each switch is represented as a vector and they are projected in space to form a hexagon with six sectors which are equally divided as shown in Fig.5 [10]. The six voltage vectors are represented as V_1, V_2, V_3, V_4, V_5, V_6. These six vectors are called as the active vectors and there are another two vectors V_0, V_7 merely called as zero vectors. Thus the presence of zero vectors makes SVM to be unique control algorithm compared other pulse width modulation methods. Fig.6 shows the space vector of voltages across the switches [15].

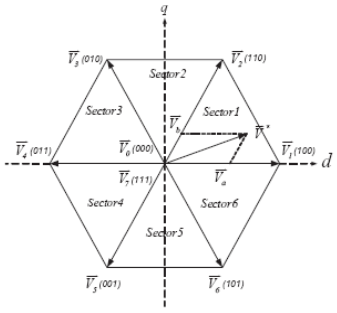

Fig.5. Projection of voltage vector

Consider, for example state V_2 space vector of voltage V_2 is

$$\bar{V}_2 = \frac{2}{3}\left[\frac{V_{DC}}{3} + a\frac{V_{DC}}{3} - a^2\frac{2V_{DC}}{3}\right] = \frac{2}{3}V_{DC}\cdot e^{j\frac{\pi}{3}} \qquad (5)$$

$$v_{no} = \frac{1}{2}median\left(v_{an}, v_{bn}, v_{cn}\right) \qquad (6)$$

Double edge modulation of reference voltage *Vao*, *Vbo* and *Vco* are equal

$$v_{ao} = v_{an} + v_{no} \qquad (7)$$

$$v_{bo} = v_{bn} + v_{no} \qquad (8)$$

$$v_{co} = v_{cn} + v_{no} \qquad (9)$$

To implement the space vector PWM, the voltage equations in the abc reference frame can be transformed into the stationary dq reference frame that consists of the horizontal (d) and vertical (q) axes depicted as shown in Fig.6.

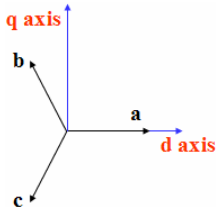

Fig.6. Representation of two reference frames

From this Fig.6, the relation between these two reference frames is shown below

$$\mathbf{f}_{dq0} = \mathbf{K}_s\mathbf{f}_{abc} \qquad (10)$$

ISSN (Print) : 2320 – 3765
ISSN (Online): 2278 – 8875

International Journal of Advanced Research in Electrical, Electronics and Instrumentation Engineering

(An ISO 3297: 2007 Certified Organization)

Vol. 4, Issue 4, April 2015

Where,

$$\mathbf{K}_s = \frac{2}{3}\begin{bmatrix} 1 & -1/2 & -1/2 \\ 0 & \sqrt{3}/2 & -\sqrt{3}/2 \\ 1/2 & 1/2 & 1/2 \end{bmatrix}, \ \mathbf{f}_{dq0}=[f_d\ f_q\ f_0]^T, \ \mathbf{f}_{abc}=[f_a\ f_b\ f_c]^T,$$

And 'f' denotes either voltage or current variable.

Therefore, space vector PWM can be implemented by the following steps:

Step 1: Determine V_d, V_q, V_{ref}, and angle (α):
From the Fig.7,

$$\begin{bmatrix} V_d \\ V_q \end{bmatrix} = \frac{2}{3}\begin{bmatrix} 1 & -\frac{1}{2} & -\frac{1}{2} \\ 0 & \frac{\sqrt{3}}{2} & -\frac{\sqrt{3}}{2} \end{bmatrix}\begin{bmatrix} V_{an} \\ V_{bn} \\ V_{cn} \end{bmatrix} \qquad (11)$$

$$\therefore \left|\overline{V}_{ref}\right| = \sqrt{V_d^{\,2} + V_q^{\,2}}$$

$$\therefore \alpha = \tan^{-1}\left(\frac{V_q}{V_d}\right) = \omega t = 2\pi f t$$

Where f= fundamental frequency.

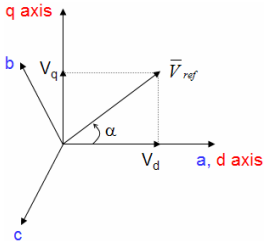

Fig.7. Representation of reference voltage in two reference frame

Step 2. Determine time duration T_1, T_2, T_0:
From the Fig.8,

$$\mathbf{T1} = \frac{\sqrt{3}\cdot T_z \cdot \left|\overline{V}ref\right|}{V_{dc}}\left(\sin\frac{n}{3}\pi\cos\alpha - \cos\frac{n}{3}\pi\sin\alpha\right) \qquad (12)$$

$$\mathbf{T2} = \frac{\sqrt{3}\cdot T_z \left|\overline{V}ref\right|}{V_{dc}}\left(-\cos\alpha\cdot\sin\frac{n-1}{3}\pi + \sin\alpha\cdot\cos\frac{n-1}{3}\pi\right) \qquad (13)$$

$$\therefore T_0 = T_z - T_1 - T_2 \qquad (14)$$

Where,

$$T_z\cdot\overline{V}_{ref} = (T_1\cdot\overline{V}_1 + T_2\cdot\overline{V}_2)$$

ISSN (Print) : 2320 – 3765
ISSN (Online): 2278 – 8875

International Journal of Advanced Research in Electrical, Electronics and Instrumentation Engineering

(An ISO 3297: 2007 Certified Organization)

Vol. 4, Issue 4, April 2015

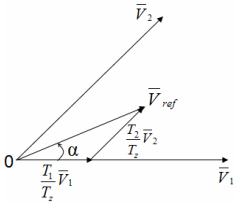

Fig.8. Representation of V_{ref}

Step 3. Determine the switching time of each MOSFET:

The switching times for the MOSFET's of the inverter are shown in the Table.1

Sector	Upper Switches (S_1, S_3, S_5)	Lower Switches (S_4, S_6, S_2)
1	$S_1 = T_1 + T_2 + T_0/2$ $S_3 = T_2 + T_0/2$ $S_5 = T_0/2$	$S_4 = T_0/2$ $S_6 = T_1 + T_0/2$ $S_2 = T_1+T_2+T_0/2$
2	$S_1 = T_1 + T_0/2$ $S_3 = T_1 + T_2 + T_0/2$ $S_5 = T_0/2$	$S_4 = T_2 + T_0/2$ $S_6 = T_0/2$ $S_2 = T_1+T_2+T_0/2$
3	$S_1 = T_0/2$ $S_3 = T_1 + T_2 + T_0/2$ $S_5 = T_2 + T_0/2$	$S_4 = T_1+T_2+T_0/2$ $S_6 = T_0/2$ $S_2 = T_1 + T_0/2$
4	$S_1 = T_0/2$ $S_3 = T_1 + T_0/2$ $S_5 = T_1 + T_2 + T_0/2$	$S_4 = T_1+T_2+T_0/2$ $S_6 = T_2 + T_0/2$ $S_2 = T_0/2$
5	$S_1 = T_2 + T_0/2$ $S_3 = T_0/2$ $S_5 = T_1 + T_2 + T_0/2$	$S_4 = T_1 + T_0/2$ $S_6 = T_1+T_2+T_0/2$ $S_2 = T_0/2$
6	$S_1 = T_1 + T_2 + T_0/2$ $S_3 = T_0/2$ $S_5 = T_1 + T_0/2$	$S_4 = T_0/2$ $S_6 = T_1+T_2+T_0/2$ $S_2 = T_2 + T_0/2$

Table.1. Switching times for the MOSFET

Thus based on the above three steps the algorithm of Space Vector Modulation is implemented and the distortion less three phase voltages are obtained [9].

VI. SIMIULATION CIRCUTS AND RESULTS

The simulations tests are carried on with the parameters of 3.5 kilowatt wind turbine system and the simulated results are displayed as follows,

A. Open loop controlled DC-DC converter

The open loop simulation of the DC-DC converter is shown in Fig.9, the response of the open loop is observed at the output for various input voltages.

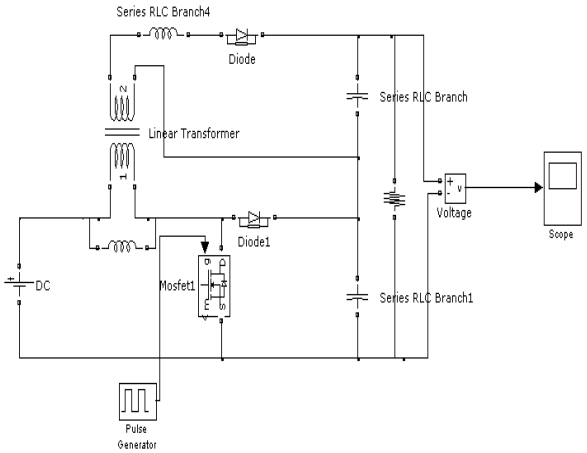

Fig.9. Step up DC-DC converter open loop

ISSN (Print) : 2320 – 3765
ISSN (Online): 2278 – 8875

International Journal of Advanced Research in Electrical, Electronics and Instrumentation Engineering

(An ISO 3297: 2007 Certified Organization)

Vol. 4, Issue 4, April 2015

Initially the input voltage is fixed as 52V and the output obtained is of 358V, after the time of 2 ms the input is decreased to 47V, now the output voltage decreases to324V. This response is shown in the Fig.10

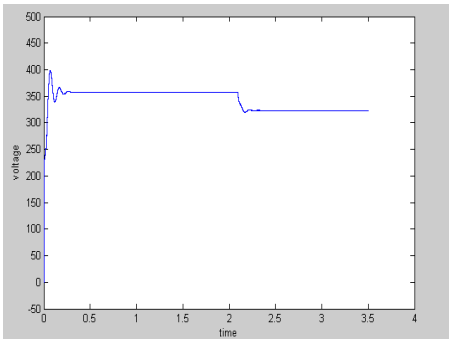

Fig.10. Output voltage waveform for the DC-DC converter open loop

B. Closed loop controlled DC-DC converter

The closed loop control of the DC-DC converter is implemented using the P and PI controller to obtain a constant DC output voltage which is shown in the Fig.11

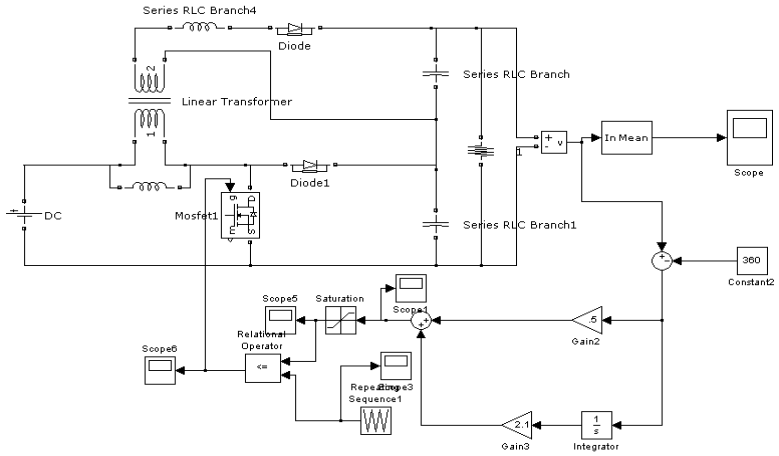

Fig.11. DC-DC converter closed loop

The response obtained with the closed loop is much better compared with the open loop for the similar changes in the input as shown in Fig.12

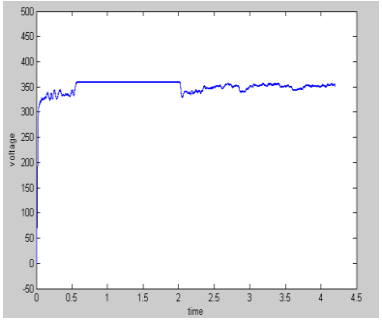

Fig.12. Output voltage waveform for the DC-DC converter closed loop

ISSN (Print) : 2320 – 3765
ISSN (Online): 2278 – 8875

International Journal of Advanced Research in Electrical, Electronics and Instrumentation Engineering

(An ISO 3297: 2007 Certified Organization)

Vol. 4, Issue 4, April 2015

C. Closed loop controlled NPC inverter (with ordinary PWM control)

The closed loop circuit of the NPC inverter is implemented using the proportional controller and the proportional integral controller as shown in the Fig.13. The desired voltage is obtained by controlling the high frequency pulses provided to the MOSFET's.

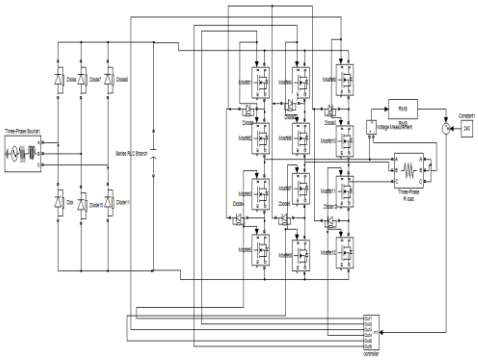

Fig.13. NPC inverter closed loop with ordinary PWM control

The output voltage waveform for the open loop NPC inverter is of high frequency square wave which is shown in the Fig.14

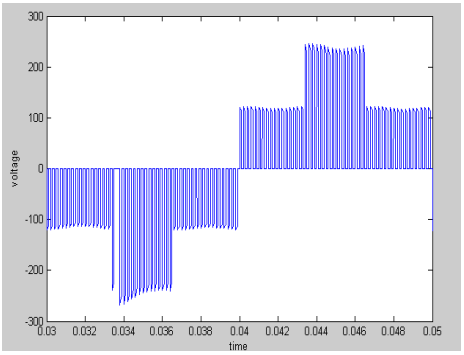

Fig.14. Output voltage waveform for NPC inverter closed loop

The FFT analysis for the above waveform shows a very high value of distortion which is shown in the Fig.15.

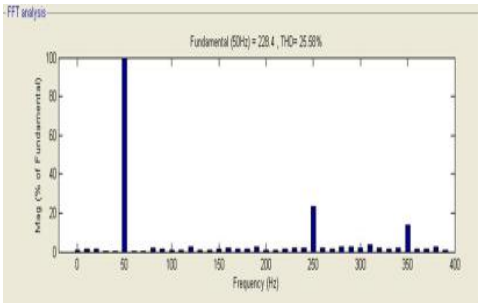

Fig.15. FFT analysis of the output voltage waveform

ISSN (Print) : 2320 – 3765
ISSN (Online): 2278 – 8875

International Journal of Advanced Research in Electrical, Electronics and Instrumentation Engineering

(An ISO 3297: 2007 Certified Organization)

Vol. 4, Issue 4, April 2015

D. Space Vector Modulation controlled NPC inverter

The Fig.16 shows the circuit model of Space Vector controlled Neutral Point Clamped Inverter operating in open loop with RLC load.

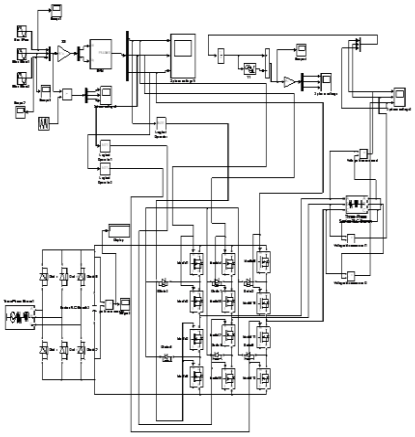

Fig.16. SVM controlled NPC inverter

The three phase voltages obtained from the SVM controlled NPC Inverter is shown in the Fig.17

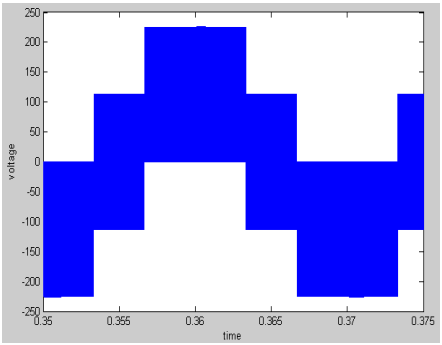

Fig.17. Output waveform for SVM controlled NPC inverter

The FFT analysis for the above waveform shown in the Fig18.

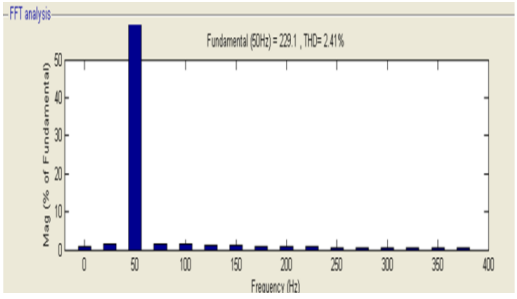

Fig.18. FFT analysis of the output voltage waveform

From the FFT analysis of both the waveform (i.e.) Fig.15 and Fig.18**,** we can conclude that the Total Harmonic Distortion for the Space Vector Modulation controlled Inverter is very less compared to the PWM technique.

ISSN (Print) : 2320 – 3765
ISSN (Online): 2278 – 8875

International Journal of Advanced Research in Electrical, Electronics and Instrumentation Engineering

(An ISO 3297: 2007 Certified Organization)

Vol. 4, Issue 4, April 2015

Thus Space Vector Modulation control forms an efficient control technique to obtain a pure, distortion less 3phase sinusoidal voltage from Inverter.

E. Converter and Inverter system

The merged circuit is a combination of rectifier, inverter and converter circuit with converter operating in closed loop is shown in the Fig.19.

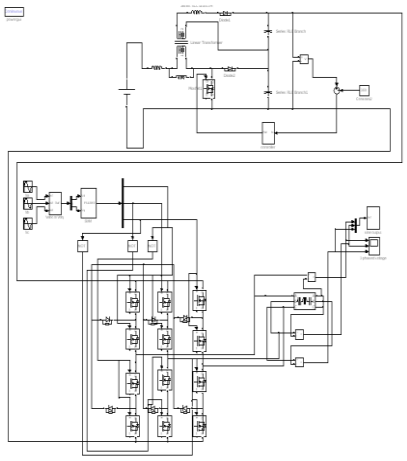

Fig.19. Inverter & Converter system

The output voltages V_a, V_b, V_c of the inverter and converter merged circuit are shown in the Fig.20

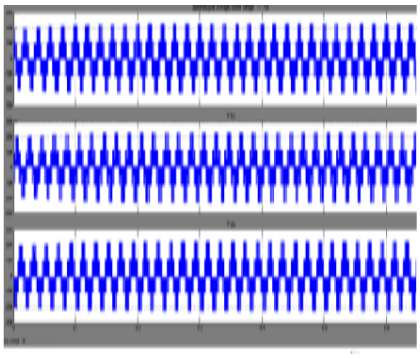

Fig.20. Output voltage waveform obtained from the converter & inverter system

VII. PROTOTYPE

The overall prototype of the combined Converter and Inverter is shown in the Fig.21. The supply for the converter is provided using the auto transformer which is rectified using rectifier and filtered using capacitor. The constant DC supply from the closed loop controlled converter is provided as a constant supply to the inverter. The space vector pulses from the PIC controller is provided to the corresponding MOSFETs of the inverter arrangement. The load used is resistive load of 1kΩ, 10watts and the three phase voltage waveform obtained is shown in the Fig.23.

ISSN (Print) : 2320 – 3765
ISSN (Online): 2278 – 8875

International Journal of Advanced Research in Electrical, Electronics and Instrumentation Engineering

(An ISO 3297: 2007 Certified Organization)

Vol. 4, Issue 4, April 2015

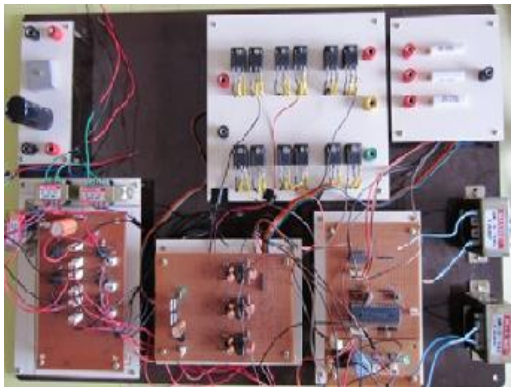

Fig.21. Prototype of the combined Converter and Inverter system

The space vector pulses generated by the PIC controller are of magnitude 5V. The pulses are generated for all the six sectors and thus these pulses are amplified and are given to the MOSFETs as gate triggering pulse. The Fig.22 shows the SVM pulses for first sector similarly the SVM pulses are obtained for all the six sectors.

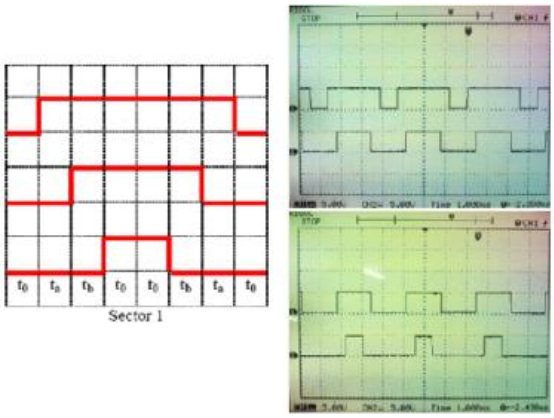

Fig.22.Space Vector Pulses obtained from PIC controller

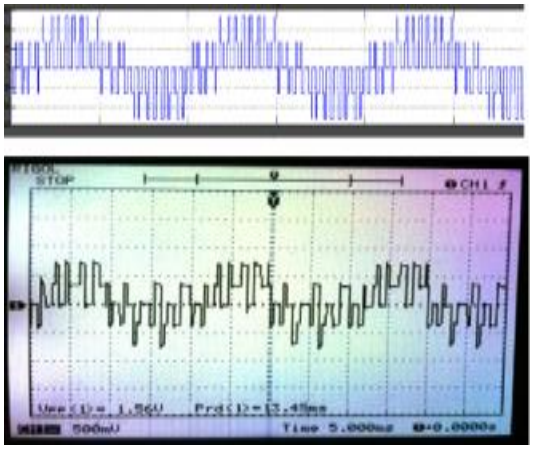

Fig.23. Output voltage waveform obtained from the prototype

ISSN (Print) : 2320 – 3765
ISSN (Online): 2278 – 8875

International Journal of Advanced Research in Electrical, Electronics and Instrumentation Engineering

(An ISO 3297: 2007 Certified Organization)

Vol. 4, Issue 4, April 2015

VIII. CONCLUSION

The performance characteristics of the open loop and the closed loop of the Converter and Neutral Point Clamped Inverter are evaluated. The simulation results of the Inverter shows that the THD obtained using the Space Vector Modulation is very much lesser compared to the ordinary Pulse width modulated inverter. The same circuit is implemented as hardware and the result shows that the output obtained using the prototype is thus similar to simulation results. Thus the Space Vector Modulation provides the near sinusoidal output voltage with very less distortion.

The converter will be implemented using neural controller in order to obtain a constant DC output voltage with variation in the input DC voltage. The prototype will be implemented in real time for roof top wind turbines and will be tested under various conditions. The data from the CWET will be used and the per day power output from this method will be compared with the present available unit.

REFERENCES

[1]Gerard Ledwich, Senior Member IEEE (2005), 'Current Source Inverter Modulation', IEEE transactions on power electronics. vol 6, no 4.
[2]Jingya Dai, Student Member, IEEE, Dewei (David) Xu, Member, IEEE, and Bin Wu, Fellow (2009), 'A Novel Control Scheme for Current-Source- Converter-Based PMSG Wind Energy Conversion Systems', IEEE transactions on power electronics, vol. 24, no. 4.
[3] Lakshmi K., Chitralekha S., Illamani V., Menezes G.A., "Prevalence of bacterial vaginal infections in pre and postmenopausal women", International Journal of Pharma and Bio Sciences, ISSN : 0975-6299, 3(4) (2012) pp.949-956.
[4] Lodrigucz, Wiechniann. E, Iloltz. J, Suirez*. A, Sepilveda. (2000), 'IGBT Inverter with Vector Modulation', EPE Journal, Vol. 2, No1.
[5] Nashiren. F, Mailah Department of Electrical and Electronic Engineering, Faculty of Engineering University Malaysia (2009), 'Neutral-Point-Clamped Multilevel Inverter Using Space Vector Modulation', European Journal of Scientific Research ISSN Vol.28 No.1, pp.82-91.
[6] Sharmila S., Jeyanthi Rebecca L., Das M.P., "Production of Biodiesel from Chaetomorpha antennina and Gracilaria corticata", Journal of Chemical and Pharmaceutical Research, ISSN : 0975 – 7384, 4(11) (2012) pp.4870-4874.
[7] Pinheiro. H, F. Botterbn, C. Rech, L. Schuch, R. F. Camargo, H. L. Hey, H. A. Griindling, J. R. Pinheiro GEPOC Federal University of Santa Maria – UFSM (2009), 'Space Vector Modulation for Voltage-Source Inverters: A Unified Approach', IEEE Trans. vol 39, pp. 410-419.
[8] Tafticht. T, Agbossou. K and Chériti. A Hydrogen Research Institute University Trois-Rivières (2006), 'DC Bus Control of Variable Speed Wind Using a Buck-Boost Converter', IEEE Tran. Power Electronics, Vol.16, Issue 3, pp. 375 – 381, May 2001.
[9] Rajkumar B., Vijay Kalimuthu B., Rajkumar R., Santhakumar A.R., "Proportioning of recycled aggregate concrete", Indian Concrete Journal, ISSN : 0019-4565, 79(10) (2005) pp.46-50.
[10] Toit Mouton. H, Member, IEEE (2002), 'Natural Balancing of Three-Level Neutral-Point-Clamped PWM Inverters', IEEE transactions on industrial electronics, vol. 49, no. 5.
[11] Tseng K.C. and Liang T.J. (2009), 'Novel high-efficiency step-up converter', IEEE Trans. Power Electron., 2001, 16, (5), pp. 649–658.
[12] Vijayaprakash S., Langeswaran K., Jagadeesan A.J., Rveathy R., Balasubramanian M.P., "Protective efficacy of Terminalia catappa L. leaves against lead induced nephrotoxicity in experimental rats", International Journal of Pharmacy and Pharmaceutical Sciences, ISSN : 0975 - 1491, 4(S3) (2012) pp.454-458.
[13] Wang. F, Senior Member, IEEE (2009), 'Sine-Triangle vs. Space Vector Modulation for Three-Level Voltage Source Inverters', GE Industrial System IEEE Annual Conference Record, pp. 595-601.
[14] Shanthi B., Revathy C., Devi A.J.M., Parameshwari P.J., Stephen T., "Serum 25(OH)D and type 2 diabetes mellitus", Journal of Clinical and Diagnostic Research, ISSN : 0973 - 709X, 6(5) (2012) pp.774-776.
[15] Xuezhi WU, Yadong LIU, Lipei Huang Dept. of Electrical Engineering**,** Tsinghua University (2008), 'A Novel Space Vector Modulation Algorithm for Three-level PWM Voltage Source Inverter', IEEE PESC, pp. 1004-1010.
[14]B Karthik, TVUK Kumar, Authentication Verification and Remote Digital Signing Based on Embedded Arm (LPC2378) Platform, World Applied Sciences Journal 19 (9), 1146-1149, 2014.
[15]Shriram, Revati; Sundhararajan, M; Daimiwal, Nivedita; , Effect of change in intensity of infrared LED on a photoplethysmogramIEEE ommunications and Signal Processing (ICCSP), 2014 International Conference on, PP 1064-1067,2014.
[16]Daimiwal, Nivedita; Sundhararajan, M; , Functional MRI Study for Eye Blinking and Finger Tapping.
[17]Daimiwal, Nivedita; Sundhararajan, M; Shriram, Revati; , Respiratory rate, heart rate and continuous measurement of BP using PPGIEEE Communications and Signal Processing (ICCSP), 2014 International Conference on, PP 999-10022014.
[18]Daimiwal, Nivedita; Sundhararajan, M; Shriram, Revati; , Non Invasive FNIR and FMRI system for Brain Mapping.
[19]Shriram, Revati; Sundhararajan, M; Daimiwal, Nivedita; , Human Brain Mapping based on COLD Signal Hemodynamic Response and Electrical NeuroimagingarXiv preprint arXiv:1307.4171, 2013